VOLUME 27 · NUMBER 16 · JUNE 1 2009

JOURNAL OF CLINICAL ONCOLOGY

ORIGINAL REPORT

[18F]Fluorodeoxyglucose Positron Emission Tomography Correlates With Akt Pathway Activity but Is Not Predictive of Clinical Outcome During mTOR Inhibitor Therapy

Wen Wee Ma, Heather Jacene, Dongweon Song, Felip Vilardell, Wells A. Messersmith, Dan Laheru, Richard Wahl, Chris Endres, Antonio Jimeno, Martin G. Pomper, and Manuel Hidalgo

From the Roswell Park Cancer Institute, Buffalo, NY; Sidney Kimmel Comprehensive Cancer Center at Johns Hopkins, Baltimore, MD; University of Colorado Cancer Center, Aurora, CO; and Centro Integral Oncologico "Clara Campal," Madrid, Spain.

Submitted June 28, 2008; accepted December 15, 2008; published online ahead of print at www.jco.org on April 20, 2009.

Supported by Grants No. R21CA112919 and U24 CA92871 from the National Cancer Institute.

Presented in part at the 44th Annual Meeting of the American Society of Clinical Oncology, May 30-June 3, 2008, Chicago, IL; and at the American Association of Cancer Research Annual Meeting, April 12-16, 2008, San Diego, CA.

Terms in blue are defined in the glossary, found at the end of this article and online at www.jco.org.

Authors' disclosures of potential conflicts of interest and author contributions are found at the end of this article.

Clinical Trials repository link available on JCO.org.

Corresponding author: Manuel Hidalgo, MD, PhD, Sidney Kimmel Comprehensive Cancer Center, Johns Hopkins University, 1650 Orleans St, Room 1M89, Baltimore, MD 21231; e-mail: mhidalg1@jhmi.edu.

0732-183X/09/2716-2697/$20.00

DOI: 10.1200/JCO.2008.18.8383

ABSTRACT

Purpose
Positron emission tomography (PET) with [18F]fluorodeoxyglucose (FDG-PET) has increasingly been used to evaluate the efficacy of anticancer agents. We investigated the role of FDG-PET as a predictive marker for response to mammalian target of rapamycin (mTOR) inhibition in advanced solid tumor patients and in murine xenograft models.

Patients and Methods
Thirty-four rapamycin-treated patients with assessable baseline and treatment FDG-PET and computed tomography scans were analyzed from two clinical trials. Clinical response was evaluated according to Response Evaluation Criteria in Solid Tumors, and FDG-PET response was evaluated by quantitative changes and European Organisation for Research and Treatment of Cancer (EORTC) criteria. Six murine xenograft tumor models were treated with temsirolimus. Small animal FDG-PET scans were performed at baseline and during treatment. The tumors were analyzed for the expression of pAkt and GLUT1.

Results
Fifty percent of patients with increased FDG-PET uptake and 46% with decreased uptake had progressive disease (PD). No objective response was observed. By EORTC criteria, the sensitivity of progressive metabolic disease on FDG-PET in predicting PD was 19%. Preclinical studies demonstrated similar findings, and FDG-PET response correlated with pAkt activation and plasma membrane GLUT1 expression.

Conclusion
FDG-PET is not predictive of proliferative response to mTOR inhibitor therapy in both clinical and preclinical studies. Our findings suggest that mTOR inhibitors suppress the formation of mTORC2 complex, resulting in the inhibition of Akt and glycolysis independent of proliferation in a subset of tumors. Changes in FDG-PET may be a pharmacodynamic marker for Akt activation during mTOR inhibitor therapy. FDG-PET may be used to identify patients with persistent Akt activation following mTOR inhibitor therapy.

J Clin Oncol 27:2697-2704. © 2009 by American Society of Clinical Oncology

INTRODUCTION

The ability to predict response to chemotherapy is a cornerstone in individualized cancer therapy. Positron emission tomography (PET) with [18F]fluorodeoxyglucose (FDG-PET) evaluates cancer cell glycolysis (Warburg effect) as a surrogate for tumor response, and early changes in FDG-PET signal were found to predict imatinib response in gastrointestinal stromal tumor (GIST).[1-4] This discovery led to much interest in using FDG-PET as predictive marker of response in the development of novel targeted anticancer agents, including inhibitors of the mammalian target of rapamycin (mTOR) protein.[5]

The Akt-mTOR pathway is perturbed in a number of human cancers as a result of aberrant events such as PTEN loss, Akt amplification, activating mutations of tuberous sclerosis complex, or constitutive activation of upstream kinases including epidermal growth factor receptor.[6] Interruption of the pathway achieves antiproliferative, antisurvival, antiangiogenic, and proapoptotic effects in preclinical studies.[7-14] Inhibitors of mTOR protein, such as temsirolimus (Torisel; Wyeth, Madison, NJ), improved the survival of patients with clear cell renal cell carcinoma and validated the pathway as a rational cancer target.[15] However, the benefit of mTOR inhibitors varies between different tumor types and

patient populations. Hence, there is a need for predictive biomarkers to better select the patient population most likely to benefit from mTOR inhibitor therapy. FDG-PET had been suggested as a noninvasive pharmacodynamic marker for target inhibition during mTOR inhibitor therapy in renal cell carcinoma.[16]

In this study, we initially hypothesized that FDG-PET response is predictive of clinical tumor response to mTOR inhibitor therapy. However, this hypothesis was refuted by the data from clinical trials at our institution showing that FDG-PET response was not predictive of tumor response to rapamycin, an mTOR inhibitor, in patients with advanced solid tumors. We attempted to study this matter further, confirming the phenomenon in murine tumor xenograft models, and investigated further the underlying relationship between the glycolytic and Akt/mTOR pathways.

PATIENTS AND METHODS

Patients, Clinical Study Design, and Treatment Plan

Clinical data and FDG-PET and computed tomography (CT) studies of patients with advanced or metastatic solid tumors treated with rapamycin in two clinical trials were collated. The utility of FDG-PET imaging as a predictive biomarker for clinical response to rapamycin was an objective for both trials. Patients were enrolled from a phase I study of rapamycin in refractory advanced solid tumor patients and a phase II trial of rapamycin in patients with gemcitabine-refractory advanced pancreatic adenocarcinoma. The results for the phase I trial were published separately, and enrollment for the phase II trial continues.[17] Rapamycin was administered orally once a day at a flat dose of 5 mg in the phase II trial and at a dose range from 2 to 9 mg in the phase I trial. The maximum-tolerated dose of rapamycin in the phase I study was determined to be 6 mg orally daily on a continuous basis. Each cycle is 28 days. Both clinical studies were approved by the institutional review board, and patients provided written informed consent before enrollment. Other eligibility criteria include age $\geq$ 18 years, measurable disease, Eastern Cooperative Oncology Group performance status $\leq$ 1, life expectancy of 12 weeks or longer, and adequate bone marrow, hepatic, and renal function. Patients who received chemotherapy or investigational drug within 1 month before the start of rapamycin therapy were not eligible. The patients were evaluated every 8 weeks for tumor response or earlier if disease progression was suspected clinically. Clinical FDG-PET/CT images were obtained before the start of the study regimen and after one cycle of therapy or at disease progression. Tumor response was reported per Response Evaluation Criteria in Solid Tumors (RECIST) criteria.[18] Time to progression (TTP) was defined as the time interval from study registration to disease progression.

Clinical FDG-PET Imaging

FDG tracer was obtained commercially (PETNet Solutions, Malvern, PA) for clinical and preclinical PET imaging. FDG-PET and CT imaging were performed with a PET/CT scanner (Discovery LS; GE Medical Systems, Waukesha, WI) before any treatment and during treatment. Patients were fasted for 6 hours or longer before imaging; 10 to 20 mCi of FDG were injected intravenously, and images were obtained 50 to 70 minutes after injection. Analysis was performed by standardized uptake value (SUV) of a 1-cm tumor area with maximal signal after visual analysis of the gross tumor and corrected for lean body mass (SUV_{max}). Up to five target lesions per patient were identified. Changes in the SUV_{max} during treatment (δSUV_{max}) were determined by the following equation: (post-treatment SUV_{max} – baseline SUV_{max})/baseline SUV_{max}, expressed in percentage. The δSUV_{max} for all target lesions were averaged ($m\delta SUV_{max}$) and reported per the 1999 European Organisation for Research and Treatment of Cancer recommendations.[19]

Preclinical Tumor Models and Treatment Plan

Six subcutaneous tumor xenograft models were developed. Four tumor models were from resected human pancreatic adenocarcinoma specimens (Panc420, Panc194, Panc294, and Panc140), and two were from pancreatic cancer cell lines (Panc1 and BxPC3); these were obtained from American Tissue Culture Collection (Manassas, VA). Six-week-old female athymic nude mice were obtained from Harlan Laboratory (Indianapolis, IN). The methodology of developing subcutaneous nude mice tumor xenograft models from resected pancreatic cancer specimens was described previously.[20] For the cancer cell line models, 5×10^6 cells in 100 μL Matrigel (BD Biosciences, Bedford, MA) was injected subcutaneously into the flanks of the nude mice. All animal protocols were approved by the Johns Hopkins University Animal Use and Care Committee and in accordance with the guidelines of the American Association of Laboratory Animal Care.

Temsirolimus was provided by Wyeth Research (Colleville, PA). Temsirolimus is a synthetic ester of rapamycin with comparable preclinical antineoplastic effects as rapamycin.[21] Therefore, no differences in drug action were expected between the two. Rapamycin is administered by oral gavages, whereas temsirolimus, which has better water solubility, can be administered intraperitoneally, ensuring more reliable drug delivery in in vivo studies.

The subcutaneous tumors were allowed to grow to a size of approximately 200 μL before being randomly assigned to receive vehicle intraperitoneally daily or temsirolimus 20 mg/kg/d intraperitoneally for 2 weeks. Tumor growth was monitored by caliper measurement and reported as the treated-to-control (T/C) ratio, which was derived as follows for each xenograft model after 2 weeks: (volume of treated tumors – volume of control tumors)/volume of control tumors. The tumors were stored as fresh frozen and paraffin-embedded specimens after harvest. FDG-PET images were obtained before the start of therapy and after 1 week of therapy.

Preclinical FDG-PET Imaging

Preclinical PET images were obtained with eXplore VISTA Pre-Clinical PET scanner (GE Medical Systems, Waukesha, WI). CT scans were performed using X-SPECT (Gamma Medica-Ideas, Northridge, CA) to correlate with PET images. The mice were fasted overnight and anesthetized with inhaled isoflurane. Fasting blood glucose level was obtained before FDG administration. Approximately 350 μCi of FDG was injected in the lateral tail vein, and residual dose in the syringe was noted to derive the actual injected dose. PET scans of the tumor-bearing mice were performed 1 hour after FDG injection. We previously validated that maximal tumor FDG uptake occurred 1 hour after injection by dynamic PET scan. The PET images were digitalized and analyzed with ImageJ (version 1.39u; National Institutes of Health, Bethesda, MD) and AMIDE (version 0.91; Andrea Loening, Stanford University, Stanford, CA).

For quantitative analysis, regions of interest (ROIs) were manually placed over the subcutaneous tumor xenografts. The FDG signal intensity for each voxel within the ROI was registered as counts, and the top one percentile of voxels are averaged and reported as maximum counts for the ROI (MaxC). The MaxC for each ROI is then corrected for the injected dose of FDG, mouse body weight, blood glucose level, and time lapsed between injection and scanning to obtain the SUV_{max} value for the ROI. The changes in FDG uptake for each tumor after treatment was reported as δSUV_{max}, which is determined by the following equation: (SUV_{max} after 1 week – SUV_{max} at baseline)/SUV_{max} at baseline. The change in FDG uptake for each treatment group was obtained by averaging δSUV_{max} of the tumors within the group and reported as $\delta SUV_{max}(av) \pm$ SEM. The $\delta SUV_{max}(av)$ of the temsirolimus-treated group was normalized to the vehicle-treated group for comparison between xenograft models. FDG uptake in mediastinum acted as control for each image.

Immunohistochemistry

Five-micrometer formalin-fixed paraffin sections were used for immunohistochemical staining according to manufacturer's instructions. GLUT1 (ab652; Abcam, Cambridge, MA) staining was performed using citrate-steam recovery. Percentage of cell membrane (0% to 100%) positive for each tumor section was scored.

Western Blot

Whole cell lysates from the tumor xenografts treated with vehicle and temsirolimus were prepared in cell lysis buffer (50 mmol/L Tris-HCl, pH 7.4; 150 mmol/L NaCl; 0.5% NP-40; 1 mmol/L phenylmethyl sulfonyl

fluoride; 1 mmol/L DTT; 20 mmol/L β-glycerol phosphate; 20 mmol/L NaF; and 1 mmol/L $NaVO_3$). Protein (100 μg) was resolved on 10% sodium dodecyl sulfate-polyacrylamide gel electrophoresis and transferred onto a nitrocellulose membrane. The membrane was blocked with 5% milk in 20 mmol/L Tris-HCl (pH 7.5), 500 mmol/L NaCl, and 0.5% Tween-20 (TBST) at room temperature for 1 hour. After incubating with primary antibodies in 5% bovine serum albumin in TBST overnight at 4°C, the membrane was washed with TBST for 15 minutes, incubated with horseradish peroxidase–conjugated secondary antibody for 1 hour at room temperature, and detected by enhanced chemiluminescence system.

Statistical Analysis

Data from the studies were summarized descriptively and analyzed by simple statistics. The relationship between variables was determined by Pearson's correlation coefficient. The *t* test was used to compare two groups, and $P < .05$ was considered significant.

RESULTS

FDG-PET Response Is Not Predictive of Tumor Response and TTP to mTOR Inhibitor Therapy in Human Patients

A total of 34 patients with assessable FDG-PET studies from both clinical trials were included in the analysis. The patients were enrolled between February 2005 and May 2007. The tumor types for these patients included pancreatic adenocarcinoma, sarcoma, colorectal cancer, neuroendocrine tumor, hepatocellular carcinoma, carcinoma of unknown primary, and others (Table 1). By RECIST and EORTC (1999) criteria for FDG-PET response, FDG-PET imaging did not correctly predict tumor response in patients treated with rapamycin.

By RECIST criteria, 16 of the 34 patients had progressive disease (PD), 18 patients had stable disease, and no partial responses (PRs) or complete responses (CRs) were observed (Table 2; Fig 1) after 2 months of rapamycin therapy. Of the 16 PD patients described, five (31%) had an increase in $m\delta SUV_{max}$ that ranged from 0% to 42%, and 11 (69%) had a decrease in $m\delta SUV_{max}$ that ranged from −1% to −49%. Of the 18 patients with stable disease, five (28%) had increased $m\delta SUV_{max}$ (2% to 43%) and 13 (72%) had decreased $m\delta SUV_{max}$ (−4% to −86%). The majority of the patients (24 of 34 patients, 71%) had a decrease in $m\delta SUV_{max}$, of whom 11 (46%) had PD. The sensitivity of increased $m\delta SUV_{max}$ in predicting PD is 50% (five of 10 patients). Similar phenomenon was observed in the subset of pancreatic cancer patients (Fig 1A). Fifteen of these patients received rapamycin 5 mg daily, whereas two others received 3 and 6 mg, respectively.

Table 1. Primary Tumor Sites of Patients With Assessable FDG-PET Scans

Tumor Site	No. of Patients (N = 34)
Pancreatic (adenocarcinoma)	17
Sarcoma	4
Colorectal	3
Neuroendocrine	3
Hepatocellular	2
Unknown primary	2
Other*	3

Abbreviations: FDG-PET, [^{18}F]fluorodeoxyglucose positron emission tomography.
*Other tumor sites include small intestine, cholangiocarcinoma, and carcinoid.

Table 2. Relationship Between RECIST Response and EORTC FDG-PET Response

	Tumor Response† (No. of patients)			
FDG-PET Response*	PD	SD	PR/CR	Total
PMD	3	1	0	4
SMD	6	10	0	16
PMR	7	7	0	14
Total	16	18	0	34

NOTE. The sensitivity of FDG-PET in predicting progressive disease in advanced solid tumors patients treated with rapamycin was 19%.
Abbreviations: RECIST, Response Evaluation Criteria in Solid Tumors; EORTC, European Organisation for Research and Treatment of Cancer; FDG-PET, [^{18}F]fluorodeoxyglucose positron emission tomography; PD, progressive disease; SD, stable disease; PR, partial response; CR, complete response; PMD, progressive metabolic disease; SMD, stable metabolic disease; PMR, progressive metabolic response.
*FDG-PET response by EORTC (1999) criteria.
†Tumor response by RECIST criteria.

The analysis of the relationship between tumor response and FDG-PET response by EORTC (1999) criteria is shown in Table 2. None of the patients with progressive metabolic response on FDG-PET imaging had CR or PR by RECIST criteria. The sensitivity of FDG-PET in predicting PD was thus 19% (three of 16 patients), whereas none of the 14 patients who had progressive metabolic response on FDG-PET had CR or PR by CT imaging.

Analysis of the relationship between FDG-PET response and TTP was performed on patients treated with a daily dose of rapamycin ≥ 5 mg and patients with pancreatic cancer and treated with the same dose (Fig 1C). The TTP of all tumor types (n = 28) ranged from 31 days (epithelioid cancer of unknown origin) to 685 days (neuroendocrine tumor). Sixteen patients (57%) had a decrease in mean SUV_{max} by more than 10%, five patients (18%) had an increase by more than 10%, and seven patients (25%) had no significant changes. The TTP of patients with pancreatic cancer (n = 16) ranged from 35 to 148 days. The FDG-PET response did not correlate with TTP in these patients ($r = -0.274$ for all patients; $r = 0.072$ for pancreatic cancer patients).

Preclinical FDG-PET Response Does Not Correlate With Tumor Growth Response to mTOR Inhibitor Therapy in Nude Mice Tumor Xenograft Models

The preclinical FDG-PET studies defined three phenotypically distinct groups among the six tumor xenograft models, as follows: growth resistant (GR)/PET nonresponder (PET-R; Panc420 and Panc194), GR/PET responder (PET-S; Panc294 and Panc1), and growth sensitive (GS)/PET-S (Panc140 and BxPC3). When treated with temsirolimus, Panc420, Panc194, Panc294, and Panc1 xenograft models continued to grow after therapy (Fig 2A), with T/C ratios of 0.31, 0.52, 0.56, and 0.63, respectively (GR tumor models). The temsirolimus-treated tumors Panc140 and BxPC3 decreased to less than baseline size after 2 weeks of therapy, with T/C ratios of −0.06 and −0.06, respectively (GS tumor models).

Among the GR tumors, the SUV_{max} of temsirolimus-treated tumors of Panc420 and Panc194 increased (PET-R), whereas the SUV_{max} of Panc294 and Panc1 decreased (PET-S) after 2 weeks of therapy (Fig 2B). Quantitatively, $\delta SUV_{max}(av)$ values for Panc420, Panc194, Pan294, and Panc1 temsirolimus-treated groups were

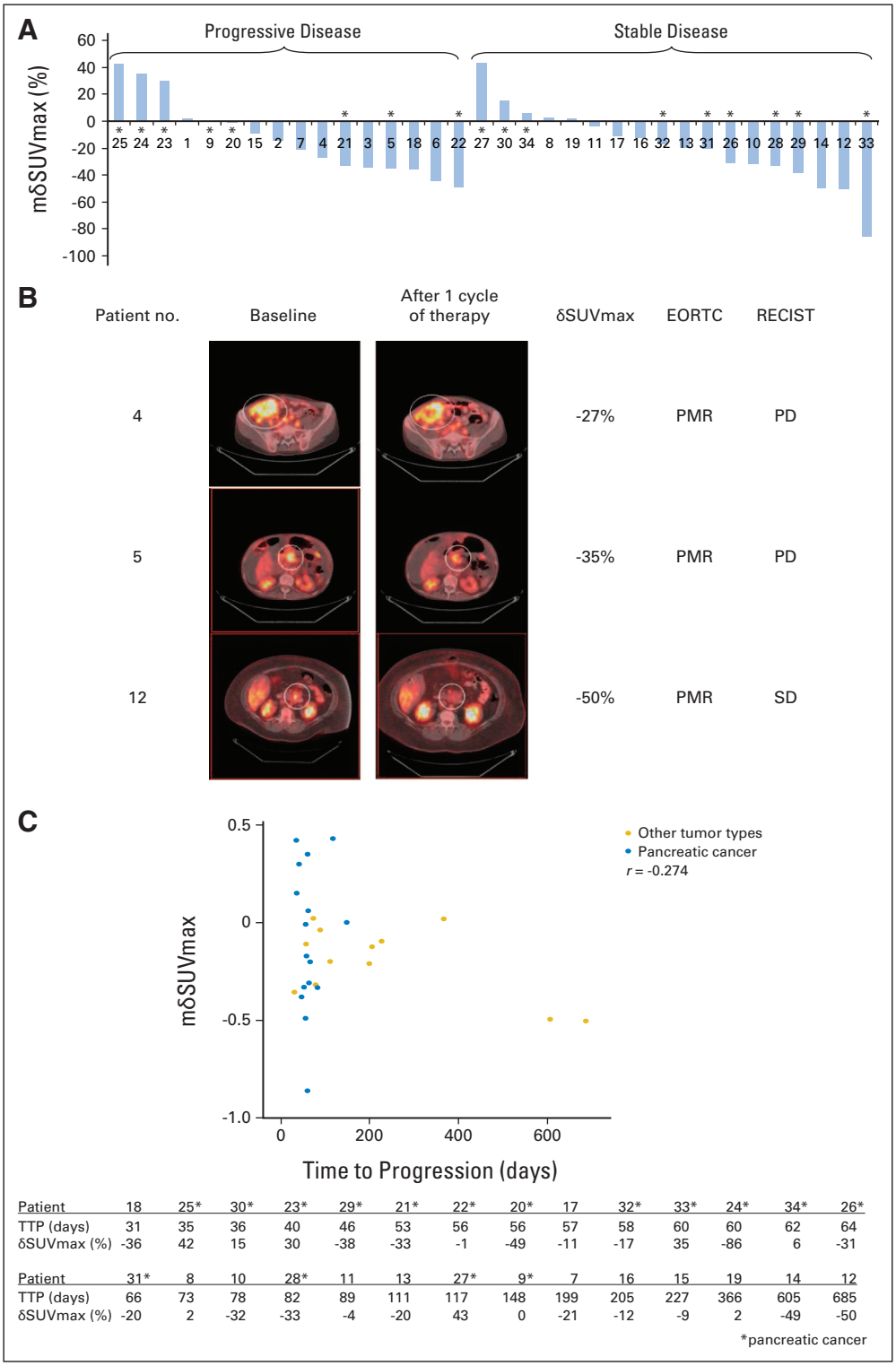

Patient	18	25*	30*	23*	29*	21*	22*	20*	17	32*	33*	24*	34*	26*
TTP (days)	31	35	36	40	46	53	56	56	57	58	60	60	62	64
δSUVmax (%)	-36	42	15	30	-38	-33	-1	-49	-11	-17	35	-86	6	-31

Patient	31*	8	10	28*	11	13	27*	9*	7	16	15	19	14	12
TTP (days)	66	73	78	82	89	111	117	148	199	205	227	366	605	685
δSUVmax (%)	-20	2	-32	-33	-4	-20	43	0	-21	-12	-9	2	-49	-50

*pancreatic cancer

Fig 1. [^{18}F]Fluorodeoxyglucose positron emission tomography (FDG-PET) response was not predictive of clinical tumor response and time to progression (TTP) to rapamycin therapy in patients. Tumor response was defined by Response Evaluation Criteria in Solid Tumors (RECIST) criteria, and FDG-PET response was defined by European Organisation for Research and Treatment of Cancer (EORTC; 1999) criteria. TTP was defined as time interval from study registration to disease progression. (A) Waterfall plot of mean change in maximum standardized uptake value (mδSUV$_{max}$) in 34 patients with assessable FDG-PET scans showing that changes in mSUV$_{max}$ did not correlate with tumor response. Patients with pancreatic cancer are marked with an asterisk (*). Deidentified patient numbers are listed on the *x*-axis for reference to patients discussed in B. (B) FDG-PET/computed tomography images of selected patients at baseline and after one cycle of rapamycin therapy. White circles denote the target lesions. Patient 4 had desmoplastic small round cell tumor, and patient 5 had pancreatic adenocarcinoma. Both had progressive disease (PD) but partial metabolic response (PMR) on FDG-PET. Patient 12 had neuroendocrine tumor of the pancreas, and had stable disease (SD), but PMR (C) Scatter plot of mδSUV$_{max}$ in patients from A treated with rapamycin $\geq$ 5 mg daily dose (n = 28). The changes in mSUV$_{max}$ did not correlate with TTP ($r = -0.274$ for all patients; $r = 0.072$ for pancreatic cancer patients). Patients with pancreatic cancer are marked with an asterisk (*). The table shows the TTP and mδSUV$_{max}$ of corresponding patients.

139% ± 98%, 123% ± 12%, −151% ± 46%, and −16% ± 7%, respectively, when compared with controls ($P < .05$). Among the GS models, the SUV$_{max}$ of the temsirolimus-treated tumors of Panc140 and BxPC3 decreased (PET-S) after 2 weeks of therapy, and the δSUV$_{max}$(*av*) values were −35% ± 12% and −108% ± 40%, respectively, when compared with controls ($P < .05$).

pAkt$_{ser473}$ and Cell Membrane–Bound GLUT1 Expression Correlates With FDG-PET Response During mTOR Inhibitor Therapy

Tumors with representative FDG-PET response phenotype of each model were analyzed qualitatively for molecular marker expression. pAkt$_{ser473}$ expression was found to correlate with FDG-PET

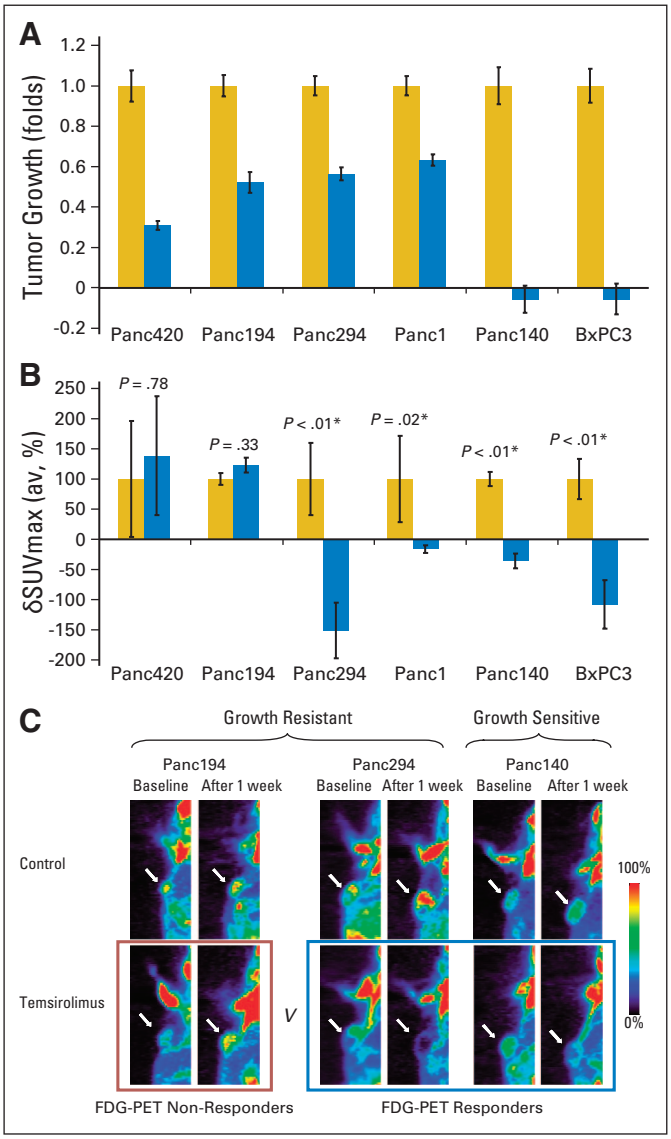

Fig 2. [^{18}F]Fluorodeoxyglucose positron emission tomography (FDG-PET) response was not predictive of tumor growth response in nude mice xenograft models. (A) Growth of tumor xenografts after 2 weeks of therapy (n = 8 tumors in each treatment group). Tumor volume was measured by caliper for 2 weeks and reported as mean ± SEM. Growths of the temsirolimus-treated tumors (blue bars) are normalized to vehicle-treated tumors (yellow bars) for each xenograft model. The tumor models resistant to temsirolimus (growth resistant [GR]) were Panc420, Panc194, Panc294, and Panc1, and the sensitive models (growth sensitive [GS]) were Panc140 and BxPC3. (B) Quantitative changes in FDG-PET signal of the vehicle-treated (yellow bars) and temsirolimus-treated (blue bars) groups for each xenograft models (n = 6 tumors in each group). Change in maximum standardized uptake value (δSUV_{max}) was determined, and $\delta SUV_{max}(av)$ for each treatment group was derived by averaging the δSUV_{max} of all the tumors within the group (reported with SEM). $\delta SUV_{max}(av)$ of temsirolimus-treated group was normalized to the vehicle-treated group for comparison between xenograft models. $\delta SUV_{max}(av)$ values of two of the temsirolimus-resistant xenograft models (Panc420 and Panc194) increased but were not statistically significant compared with controls. Compared with respective controls, the $\delta SUV_{max}(av)$ values of the other two temsirolimus-resistant xenograft models (Panc 294 and Panc1) and the two temsirolimus-sensitive xenograft models (Panc140 and BxPC3) decreased after 1 week of temsirolimus treatment compared with controls ($P < .05$). (C) Representative FDG-PET images of the xenograft models. Small animal FDG-PET images were obtained at baseline and after 1 week of vehicle or temsirolimus treatment. The size of temsirolimus-treated Panc194 and Panc294 tumors continued to grow (GR), whereas the size of Panc140 tumors decreased (GS) after 2 weeks of therapy. The FDG-PET signal in the temsirolimus-treated Panc194 tumors continued to increase (FDG-PET nonresponders), whereas that for Panc294 and Panc140 decreased (FDG-PET responders) after 1 week of therapy.

response but not growth response to temsirolimus therapy. For tumors with positive δSUV_{max} (GR/PET-R group), $pAkt_{ser473}$ expression in temsirolimus-treated Panc420 tumor was not significantly different from control, whereas $pAkt_{ser473}$ expression for Panc194 tumor was more intense (Fig 3A). $pAkt_{ser473}$ expression was less intense in tumors with negative δSUV_{max} (GR/PET-S and GS/PET-S groups) compared with controls. The Western blots were performed in triplicate and by different personnel to confirm the results. However, meaningful statistical analysis could not be performed because of the small number of tumors tested for $pAkt_{ser473}$ expression.

Increased GLUT1 expression on cell membrane was reported to be associated with increased FDG uptake.[22] Thus, we investigated the relationship between FDG-PET response to temsirolimus therapy and GLUT1 expression on tumor cell membrane by immunohistochemistry (Figs 3B and 3C). Quantitatively, the percentage of tumor cell membrane that stained positive for GLUT1 was higher in the temsirolimus-treated group than in the control group in the PET-R models (Panc420 and Panc194), whereas the percentage was lower for the PET-S models (Panc294, Panc1, Panc140, and BxPC3).

DISCUSSION

The ability to predict response to cancer treatment is a key aspect for successful individualized cancer therapy. Our understanding of the role of functional imaging techniques, such as FDG-PET, as predictive markers for response to novel targeted agents is still in the nascent stage. In this study, we attempted to define the role of FDG-PET imaging in predicting the response of cancer patients to mTOR inhibitors. The results show that early FDG-PET response is not predictive of clinical response to mTOR inhibitor therapy. Instead, FDG-PET imaging may be a novel pharmacodynamic biomarker for Akt activation during mTOR inhibitor therapy, which is not necessarily reflective of proliferative response.

Akt has pleiotropic effects important to tumorigenesis and maintenance of malignant phenotype.[23] In two glioblastoma cell lines of similar proliferation but different glucose utilization rate, Elstrom et al[24] showed that Akt activation was correlated with a higher rate of aerobic glycolysis and that disruption of the PI3k/Akt pathway inhibits glycolysis. They concluded that Akt activation promotes glucose utilization independent of any effects Akt has on stimulation of cell proliferation. Later, Tarn et al[25] reported that the therapeutic effects of imatinib on GIST cells is independent of Akt activity and glucose metabolism when they observed that in vitro constitutive activation of Akt overcame imatinib-induced blockade of glucose uptake but did not rescue GIST cells from imatinib-induced apoptosis. Together with our data, we propose that Akt is a watershed cellular signaling node from which cellular glucose metabolism can be modulated independently of proliferation in certain cancer cell types. Admittedly, our data is hypothesis generating in nature because of the small number of tumors analyzed.

Mechanistically, Akt activation causes increased transcription and plasma membrane localization of GLUT1; membrane-bound GLUT1 is an important mediator of FDG uptake in most cancer cells.[22,23] The immunohistochemistry studies for the GR/PET-S tumors (Panc294 and Panc1) showed decreased GLUT1 staining in both

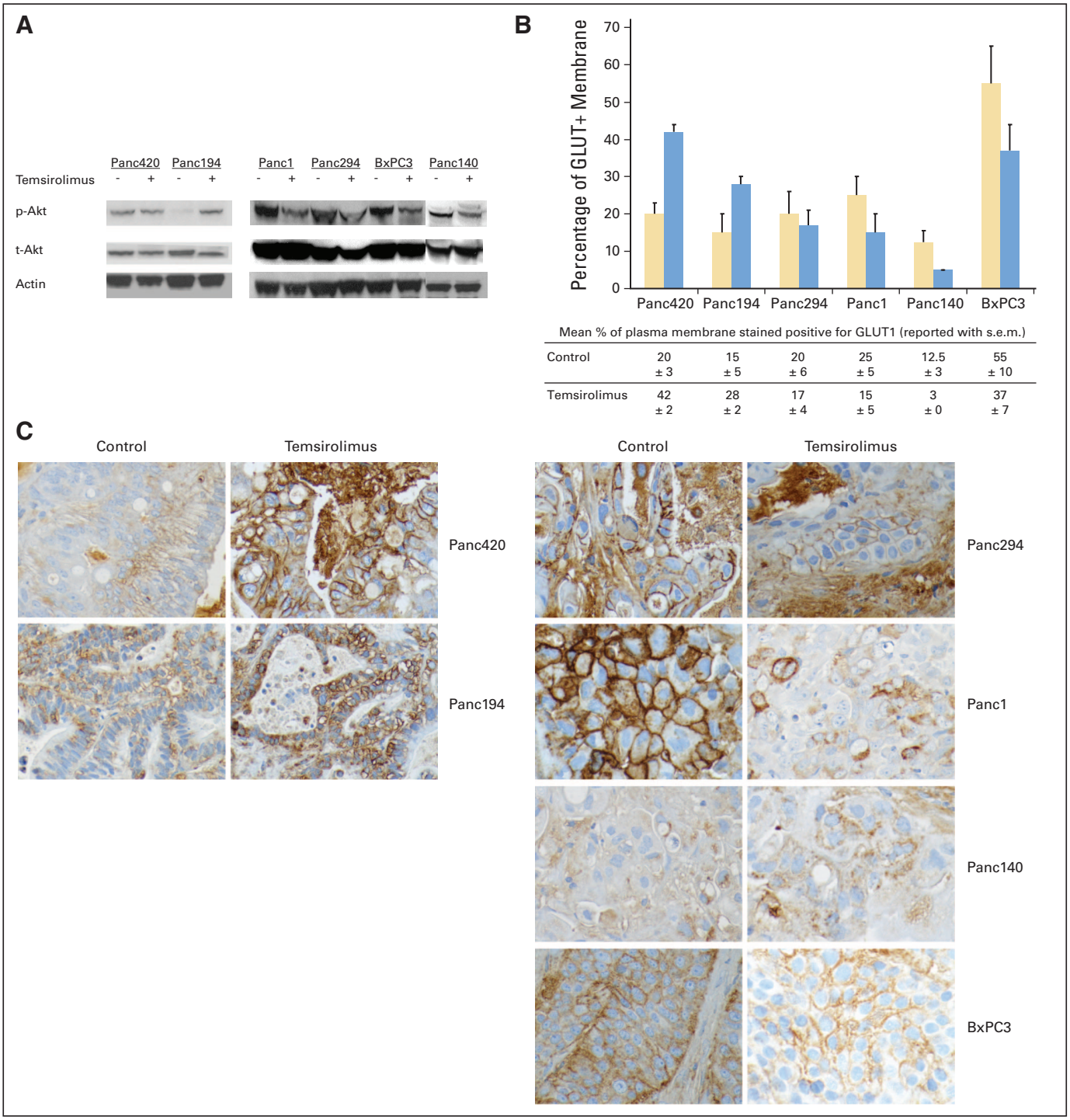

Fig 3. Changes in tumor biomarkers in response to temsirolimus and vehicle treatment. Subcutaneous tumor xenografts were harvested after 2 weeks of therapy and stored as fresh frozen and paraffin-embedded specimens. (A) Western blots of the tumors for the expression of $pAkt_{ser473}$, total Akt, and actin. The experiment was performed in triplicate. $pAkt_{ser473}$ expression correlated with changes in [^{18}F]fluorodeoxyglucose positron emission tomography (FDG-PET) signal for the tested tumors. Compared with controls, $pAkt_{ser473}$ expression was stable (Panc420) and increased (Panc194) in all xenografts with increased change in maximum standardized uptake value (δSUV_{max}) during therapy; whereas $pAkt_{ser473}$ expression decreased in all xenografts with decreased δSUV_{max} during therapy (Panc1, Panc 294, BxPC3, and Panc140). (B) Quantitative assessment of the proportion of cell membrane that stained positive for GLUT1 (n = 3 in each treatment group). GLUT1 percent membrane score is higher in temsirolimus-treated than vehicle-treated tumors in the xenograft models with positive δSUV_{max}(*av*) (Panc420 and Panc194), whereas the score is lower in the xenograft models with negative δSUV_{max}(*av*) (Panc294, Panc1, Panc140, and BxPC3). (C) Immunohistochemical staining for GLUT1 of paraffin-embedded tumor specimens. In the models with positive δSUV_{max} during therapy (Panc420 and Panc194), the percentage of cell membrane that stained positive for GLUT1 was higher in temsirolimus-treated tumors than controls. In the models with negative δSUV_{max} during therapy (Panc294, Panc1, Panc140, and BxPC3), the percentage of cell membrane that stained positive for GLUT1 was lower in temsirolimus-treated tumors than controls. To note, cytosolic GLUT1 staining in temsirolimus-treated Panc140 and BxPC3 was higher than in controls, although the percentage of cell membrane that stained positive for GLUT1 was less than in controls.

cytosol and plasma membrane, indicating that Akt inhibition inactivates GLUT1 transcription in this group of tumors during temsirolimus treatment. Whereas, the immunohistochemistry studies for the GS/PET-S tumors (Panc140 and BxPC3) showed higher a cytosolic-to-membrane ratio of GLUT1 stain in the temsirolimus-treated tumors than controls, suggesting that Akt inhibition disrupts the translocation of GLUT1 to plasma membrane to a greater extent than GLUT1 transcription in this group of tumors. Therefore, we propose that Akt inhibition cause disruption to GLUT1 transcription and/or translocation to plasma membrane in PET-S tumors.

mTOR complexes with the raptor and rictor proteins to form mTOR complex 1 (mTORC1) and mTORC2, respectively.[26] mTORC1 is susceptible to inhibition by rapamycin analogs (rapalogs) and regulates growth and cell cycle progression via downstream mediators such as p70S6k and 4E-BP1. mTORC2 is part of the upstream PI3k/Akt pathway and regulates Akt activity. mTORC2 was thought to be resistant to the action of rapalogs, but recent evidence showed that the formation of the mTORC2 complex can be inhibited by rapalogs in a cell type– and time-dependant manner.[27-29] The inhibition of Akt observed in our study is likely to be a result of the inhibition of mTORC2 formation by prolonged mTOR inhibitor exposure. We speculate that FDG-PET during mTOR inhibitor therapy can be used as a pharmacodynamic biomarker for the activity of the PI3k/Akt pathway and help select patients with the GR/PET-R phenotype who may benefit from subsequent upstream inhibition with agents such as inhibitors of PI3k and insulin-like growth factor 1 receptor.

This report highlights the fact that early changes in tumor glucose uptake may not be predictive of response to therapy for certain anticancer agents. Our study provides insight into the relationship between the Akt/mTOR pathway and glycolysis and raises the importance of validating novel imaging techniques in therapy development preclinically before integrating them into clinical practice.

AUTHORS' DISCLOSURES OF POTENTIAL CONFLICTS OF INTEREST

The author(s) indicated no potential conflicts of interest.

AUTHOR CONTRIBUTIONS

Conception and design: Wen Wee Ma, Wells A. Messersmith, Antonio Jimeno, Martin G. Pomper, Manuel Hidalgo
Financial support: Manuel Hidalgo
Administrative support: Manuel Hidalgo
Provision of study materials or patients: Wen Wee Ma, Heather Jacene, Dongweon Song, Felip Vilardell, Wells A. Messersmith, Dan Laheru, Richard Wahl, Antonio Jimeno, Manuel Hidalgo
Collection and assembly of data: Wen Wee Ma, Heather Jacene, Dongweon Song, Felip Vilardell, Dan Laheru, Chris Endres, Antonio Jimeno
Data analysis and interpretation: Wen Wee Ma, Heather Jacene, Dongweon Song, Felip Vilardell, Wells A. Messersmith, Chris Endres, Antonio Jimeno, Martin G. Pomper, Manuel Hidalgo
Manuscript writing: Wen Wee Ma, Heather Jacene, Dongweon Song, Felip Vilardell, Wells A. Messersmith, Dan Laheru, Richard Wahl, Chris Endres, Antonio Jimeno, Martin G. Pomper, Manuel Hidalgo
Final approval of manuscript: Wen Wee Ma, Heather Jacene, Dongweon Song, Felip Vilardell, Wells A. Messersmith, Dan Laheru, Richard Wahl, Chris Endres, Antonio Jimeno, Martin G. Pomper, Manuel Hidalgo

REFERENCES

1. Demetri GD, von Mehren M, Blanke CD, et al: Efficacy and safety of imatinib mesylate in advanced gastrointestinal stromal tumors. N Engl J Med 347: 472-480, 2002
2. Van den Abbeele AD, Badawi RD: Use of positron emission tomography in oncology and its potential role to assess response to imatinib mesylate therapy in gastrointestinal stromal tumors (GISTs). Eur J Cancer 38:S60-S65, 2002 (suppl 5)
3. Stroobants S, Goeminne J, Seegers M, et al: 18FDG-Positron emission tomography for the early prediction of response in advanced soft tissue sarcoma treated with imatinib mesylate (Glivec). Eur J Cancer 39:2012-2020, 2003
4. Heinicke T, Wardelmann E, Sauerbruch T, et al: Very early detection of response to imatinib mesylate therapy of gastrointestinal stromal tumours using 18fluoro-deoxyglucose-positron emission tomography. Anticancer Res 25:4591-4594, 2005
5. Dimitrakopoulou-Strauss A, Hohenberger P, Strobel P, et al: A recent application of fluoro-18-deoxyglucose positron emission tomography, treatment monitoring with a mammalian target of rapamycin inhibitor: An example of a patient with a desmoplastic small round cell tumor. Hell J Nucl Med 10:77-79, 2007
6. Granville CA, Memmott RM, Gills JJ, et al: Handicapping the race to develop inhibitors of the phosphoinositide 3-kinase/Akt/mammalian target of rapamycin pathway. Clin Cancer Res 12:679-689, 2006
7. Balsara BR, Pei J, Mitsuuchi Y, et al: Frequent activation of AKT in non-small cell lung carcinomas and preneoplastic bronchial lesions. Carcinogenesis 25:2053-2059, 2004
8. Fiala ES, Sohn OS, Wang CX, et al: Induction of preneoplastic lung lesions in guinea pigs by cigarette smoke inhalation and their exacerbation by high dietary levels of vitamins C and E. Carcinogenesis 26:605-612, 2005
9. Li J, Davidson G, Huang Y, et al: Nickel compounds act through phosphatidylinositol-3-kinase/Akt-dependent, p70(S6k)-independent pathway to induce hypoxia inducible factor transactivation and Cap43 expression in mouse epidermal Cl41 cells. Cancer Res 64:94-101, 2004
10. Segrelles C, Ruiz S, Perez P, et al: Functional roles of Akt signaling in mouse skin tumorigenesis. Oncogene 21:53-64, 2002
11. Asano T, Yao Y, Zhu J, et al: The rapamycin analog CCI-779 is a potent inhibitor of pancreatic cancer cell proliferation. Biochem Biophys Res Commun 331:295-302, 2005
12. Lieberthal W, Fuhro R, Andry CC, et al: Rapamycin impairs recovery from acute renal failure: Role of cell-cycle arrest and apoptosis of tubular cells. Am J Physiol Renal Physiol 281:F693-F706, 2001
13. Guba M, von Breitenbuch P, Steinbauer M, et al: Rapamycin inhibits primary and metastatic tumor growth by antiangiogenesis: Involvement of vascular endothelial growth factor. Nat Med 8:128-135, 2002
14. Suhara T, Mano T, Oliveira BE, et al: Phosphatidylinositol 3-kinase/Akt signaling controls endothelial cell sensitivity to Fas-mediated apoptosis via regulation of FLICE-inhibitory protein (FLIP). Circ Res 89:13-19, 2001
15. Hudes G, Carducci M, Tomczak P, et al: Temsirolimus, interferon alfa, or both for advanced renal-cell carcinoma. N Engl J Med 356:2271-2281, 2007
16. Thomas GV, Tran C, Mellinghoff IK, et al: Hypoxia-inducible factor determines sensitivity to inhibitors of mTOR in kidney cancer. Nat Med 12: 122-127, 2006
17. Jimeno A, Rudek MA, Kulesza P, et al: Pharmacodynamic-guided modified continuous reassessment method-based, dose-finding study of rapamycin in adult patients with solid tumors. J Clin Oncol 26:4172-4179, 2008
18. Therasse P, Arbuck SG, Eisenhauer EA, et al: New guidelines to evaluate the response to treatment in solid tumors: European Organization for Research and Treatment of Cancer, National Cancer Institute of the United States, National Cancer Institute of Canada. J Natl Cancer Inst 92:205-216, 2000
19. Young H, Baum R, Cremerius U, et al: Measurement of clinical and subclinical tumour response using [18F]-fluorodeoxyglucose and positron emission tomography: Review and 1999 EORTC recommendations—European Organization for Research and Treatment of Cancer (EORTC) PET Study Group. Eur J Cancer 35:1773-1782, 1999
20. Rubio-Viqueira B, Jimeno A, Cusatis G, et al: An in vivo platform for translational drug development in pancreatic cancer. Clin Cancer Res 12:4652-4661, 2006
21. Ma WW, Jimeno A: Temsirolimus. Drugs Today (Barc) 43:659-669, 2007

22. Brown RS, Goodman TM, Zasadny KR, et al: Expression of hexokinase II and Glut-1 in untreated human breast cancer. Nucl Med Biol 29:443-453, 2002

23. Plas DR, Thompson CB: Akt-dependent transformation: There is more to growth than just surviving. Oncogene 24:7435-7442, 2005

24. Elstrom RL, Bauer DE, Buzzai M, et al: Akt stimulates aerobic glycolysis in cancer cells. Cancer Res 64:3892-3899, 2004

25. Tarn C, Skorobogatko YV, Taguchi T, et al: Therapeutic effect of imatinib in gastrointestinal stromal tumors: AKT signaling dependent and independent mechanisms. Cancer Res 66:5477-5486, 2006

26. Sabatini DM: MTOR and cancer: Insights into a complex relationship. Nat Rev Cancer 6:729-734, 2006

27. Jacinto E, Loewith R, Schmidt A, et al: Mammalian TOR complex 2 controls the actin cytoskeleton and is rapamycin insensitive. Nat Cell Biol 6:1122-1128, 2004

28. Sarbassov DD, Ali SM, Sengupta S, et al: Prolonged rapamycin treatment inhibits mTORC2 assembly and Akt/PKB. Mol Cell 22:159-168, 2006

29. Zeng Z, Sarbassov Dos D, Samudio IJ, et al: Rapamycin derivatives reduce mTORC2 signaling and inhibit AKT activation in AML. Blood 109:3509-3512, 2007

Glossary Terms

mTOR: The mammalian target of rapamycin belongs to a protein complex (along with raptor and GL) that is used by cells to sense nutrients in the environment. mTOR is a serine/threonine kinase that is activated by Akt and regulates protein synthesis on the basis of nutrient availability. It was discovered when rapamycin, a drug used in transplantation, was shown to block cell growth presumably by blocking the action of mTOR.

FDG-PET: Positron emission tomography with the glucose analog [18F]fluorodeoxyglucose.

Akt pathway: A signal transduction pathway involving the signaling molecules phosphatidylinositol-3 kinase (PI3K) and Akt, where PI3K generates phosphorylated inositides at the cell membrane which are required for the recruitment and activation of Akt, a transforming serine-threonine kinase involved in cell survival.

Temsirolimus: Also called CCI-779, temsirolimus is an inhibitor of mTOR, a member of the phosphoinositide kinase-related family proteins.

Rapamycin: Also called Sirolimus, it is a potent immunosuppressant used in transplantation and inhibits cell cycle progression, preventing cell proliferation.

Glycolysis: The enzymatic breakdown of a carbohydrate (as glucose or glycogen) with the production of pyruvic acid or lactic acid and the release of energy stored in the high-energy phosphate bonds of ATP.

GLUT1: The glucose transporter type 1 is ubiquitously expressed that is important for constitutive, basal glucose transport. The transporter is widely distributed in fetal tissues, and predominantly expressed in endothelial cells, erythrocytes, and blood brain barrier in adults. The GLUT1 is found to be an important mediator of glucose influx in most cancer cells and the increased expression enables cancer cells to maintain high growth rates and metabolic activity.

mTORC1: The mTOR Complex 1 is composed of mTOR, regulatory associated protein of mTOR (raptor), and mLST8/GL). This complex has the classic features of mTOR by functioning as a sensor for nutrients and energy, and controls protein synthesis. The complex is downstream to Akt and phosphorylates S6K1 upon activation.

mTORC2: The mTOR Complex 2 is composed of mTOR, rapamycin-insensitive companion of mTOR (rictor), GL, and mSIN1. Phosphorylation of the complex stimulates Akt phosphorylation at a threonine residue that leads to full Akt activation.

